A Spatially Distributed Multi-Period Optimal Power Flow with Distributed Battery Units

Aryan Ritwajeet Jha∗, *SIEEE*, Subho Paul†, *MIEEE*, Anamika Dubey∗, *SMIEEE*
∗*School of Electrical Engineering & Computer Science*, *Washington State University*, Pullman, WA
†*Department of Electrical Engineering*, *Indian Institute of Technology Varanasi (BHU)*, Varanasi, India
∗{aryan.jha, anamika.dubey}@wsu.edu, †{subho.eee}@itbhu.ac.in

***Abstract*—~~Decrease title length (within two lines)~~ insert abstract here**

***Index Terms*—Batteries, distribution network, distributed energy resources (DERs), equivalent network approximation (ENApp)**

I. Introduction

A. Background and Prior Arts

Presently, optimal power flow (OPF) tools are developed to run the MV/LV distribution grids in the most economical, reliable, and secure manner. The usefulness of OPF studies is gaining more interest due to the penetration of distributed energy resources (DERs), especially solar photovoltaic panels. Power generation from these DERs is influenced by the weather conditions, hence highly intermittent. Presently, deployment of battery units is becoming more pertinent to mitigate the uncertainty effect and maintain the power balance by controlling the charging and/or discharging operations [1]. However, the inclusion of batteries converts the conventional single-period time-decoupled OPF problem into a multi-period time-coupled OPF analysis.

Traditionally, centralized OPF (COPF) methods were popular where grid-edge data are accumulated at a central controller location [2]. The central controller is responsible for processing the accumulated data, solving the OPF algorithm, and dispatching control signals to the controlling resources. The centralized OPF algorithms are generally developed as a mixed integer non-convex programming (MINCP) problem and then simplified either as a convex problem by adopting second-order cone programming (SOCP) relaxations [3] [4], or as a linear problem by adopting Taylor series expansion [2], polyhedral approximations [5] or linear power flow models [6].

To overcome the scalability issues related to the COPF methods, distributed OPF (DOPF) algorithms are often proposed by decomposing the original COPF problem into multiple sub-problems, solved in parallel by permitting neighborhood communication. In this regard, the Auxiliary Problem Principle (APP) and the Alternating direction method of multipliers (ADMM) are two popular algorithms used to solve

Fazio et al. [7] used the Auxiliary Problem Principle (APP) based DOPF to minimize the voltage deviation by segregating the entire distribution network into multiple voltage control zones. The non-convex problem is relaxed and solved as quadratic convex programming. Alternating direction method of multipliers (ADMM) based DOPF is proposed in [8] for determining the reactive power dispatch schedules for capacitor banks and static VAR compensators. The original non-convex problem is solved by adopting SOCP relaxation. Another ADMM based semidefinite programming (SDP) relaxed DOPF portfolio is designed in [9] for an AC network having only wind generators. Biswas et al. [10] also used SDP relaxation to develop DOPF algorithms using vanilla and accelerated ADMM methods.

TABLE I: Taxonomy table for comparison

References	DERs	Batteries	Single period OPF	Multi-period OPF	Centralized OPF	Distributed OPF	Framework
[6]			✓		✓		Linear
[3]			✓		✓		Convex
[5]	✓		✓		✓		Linear
[]- []	✓			✓			✓
[], []		✓		✓			✓
[7]	✓		✓			✓	Convex (APP)
[8]- [10]	✓		✓			✓	Convex (ADMM)
[11]	✓	✓		✓	✓		Non-convex
This paper	✓	✓		✓		✓	Non-convex (ENApp)

Gabash and Li [11] propound a nonlinear centralized optimization framework to solve the multi-period active-reactive power dispatch from the battery storages and DERs in a distribution network.

Wu et al. [12] frame a multi-period optimization problem for a virtual power plants (VPPs) collocated distribution network. The original centralized multi-parametric quadratic problem is decomposed into one master and multiple sub-problems for distribution network and VPPs, respectively by utilizing the concept of Benders Decomposition.

Previously in [13], authors' research group develop a

B. Research Gaps and Contributions

A taxonomy table to compare the existing studies and the present work is provided in I.

The specific contributions are as follows:

1) The overall problem is formulated as a non-convex programming and the

II. Problem Formulation

A. Notations

In this study, the distribution network is accounted as a tree (connected graph) having N number of buses (indexed with i, j, and k) and the study is conducted for T time steps (indexed by t), each of interval length Δt. The distribution line connecting two buses i and j are denoted by ij (having resistance and reactance of r_{ij} ohm and x_{ij} ohm, respectively) and magnitude of the current flowing through the line at time t is denoted by I_{ij}^t ($l_{ij}^t = \left(I_{ij}^t\right)^2$). The voltage magnitude of bus i at time t is given by $V_i^t \in [V_{min}, V_{max}]$ ($v_i^t = (V_i^t)^2$). Apparent power demand at a node j at time t is ${s_L}_j{}^t$ ($= {p_L}_j{}^t + j{q_L}_j{}^t$). The uncontrolled active power generation from the DER present at bus j at time step t is denoted by ${p_D}_j{}^t$ and controlled reactive power dispatch from the DER inverter is ${q_D}_j{}^t$. Static capacitance attached to a node j is denoted by q_{C_j}. The apparent power flow through line ij at time step t is S_{ij}^t ($= P_{ij}^t + jQ_{ij}^t$). The battery state of charge (soc) or energy level is B_j^t. Charging and discharging active power from battery inverter (of apparent power capacity $S_{R,j}^t$) are denoted by $P_{c_j}^t$ and $P_{d_j}^t$, respectively. The total state of charge capacity of the batteries are denoted by $E_{R,j}$, and the Rated battery powers are denoted by $P_{B_{R,j}}$. The reactive power support of the battery inverter is $q_{B_j}^t$. Rated apparent powers of DERs and Batteries at node j are denoted by $S_{D_{R,j}}$ and $S_{B_{R,j}}$ respectively.

B. Centralized Multi-Period OPF with Batteries

The OPF problem given in (1) aims to minimize the cost of power borrowed from the substation for the entire horizon. The incorporation of an additional 'Battery Loss' term helps us bypass using binary (integer) constraints for modelling the operation of batteries, which would otherwise make the optimization problem harder to solve. The term still ensures the complementarity of charging and discharging operations for any battery during a particular time period [14]–[16].

$$\min \sum_{t=1}^{T} \left[C^t P_{Subs}^t + \alpha \sum_{j\in\mathcal{B}} \left\{ (1-\eta_C) P_{C_j}^t + \left(\frac{1}{\eta_D} - 1\right) P_{D_j}^t \right\} \right] \tag{1}$$

Subject to the constraints (2) to (13) given below:

$$0 = \sum_{(j,k)\in\mathcal{L}} \{P_{jk}^t\} - (P_{ij}^t - r_{ij} l_{ij}^t) - \left(P_{d_j}^t - P_{c_j}^t\right) - p_{D_j}^t + p_{L_j}^t \tag{2}$$

$$0 = \sum_{(j,k)\in\mathcal{L}} \{Q_{jk}^t\} - (Q_{ij}^t - x_{ij} l_{ij}^t) - q_{D_j}^t - q_{B_j}^t + q_{L_j}^t \tag{3}$$

$$0 = v_i^t - v_j^t - 2(r_{ij}P_{ij}^t + x_{ij}Q_{ij}^t) + \{r_{ij}^2 + x_{ij}^2\} l_{ij}^t \tag{4}$$

$$0 = (P_{ij}^t)^2 + (Q_{ij}^t)^2 - l_{ij}^t v_i^t \tag{5}$$

$$P_{Subs}^t \geq 0 \tag{6}$$

$$v_j^t \in \left[V_{min}^2, V_{max}^2\right] \tag{7}$$

$$l_{ij}^t \in \left[0, I_{R,ij}^2\right] \tag{8}$$

$$B_j^t = B_j^{t-1} + \Delta t \eta_c P_{c_j}^t - \Delta t \frac{1}{\eta_d} P_{d_j}^t \tag{9}$$

$$B_j^t \in [soc_{min} E_{R,j}, soc_{max} E_{R,j}] \tag{10}$$

$$P_{c_j}^t, P_{d_j}^t \in \left[0, P_{B_{R_j}}\right] \tag{11}$$

$$q_{B_j}^t \in \left[-\sqrt{{S_{B_{R,j}}}^2 - {P_{B_{R,j}}}^2}, \sqrt{{S_{B_{R,j}}}^2 - {P_{B_{R,j}}}^2}\right] \tag{12}$$

$$q_{D_j}^t \in \left[-\sqrt{{S_{D_{R,j}}}^2 - {p_{D_j}^t}^2}, \sqrt{{S_{D_{R,j}}}^2 - {p_{D_j}^t}^2}\right] \tag{13}$$

The distribution network is represented with the help of the branch power flow equations (2) to (5). Constraints (2) and (3) signify the active and reactive power balance at node j. The KVL equation for branch (i, j) is represented by (4), while the equation describing the relationship between current magnitude, voltage magnitude and apparent power magnitude for nodes i and j is (5). The limits of node voltage and branch current are enforced via (7) and (8). The trajectory of the state of charge of batteries versus time is given by (9) and is the only class of constraints in this paper coupling the optimal power flow problem in time. Battery charging and discharging efficiency values used in this paper are $\eta_c = 95\%$ and $\eta_d = 95\%$ literature?. For a safe and sustainable operation of the batteries based on what literature?, the state of charge B_j^t is constrained to be within some percentage limits of the rated battery soc capacity, as given in (10). In this paper, we're using $soc_{min} = 30\%$ and $soc_{max} = 95\%$. Similarly, battery charging and discharging powers should not exceed its rated power capacity, as given by (11). (12) and (13) describe the limits for two-quadrant operation of the controlled reactive power support of DERs and Batteries respectively. It may be noted that while both of these limits are non-controllable, only the limits for DERs are time-varying, due to $p_{D_j}^t$ component. For this simulation study, the limits for battery reactive support have been curtailed, i.e. the bounds of the limit have been artificially set smaller than what would be physically permissible. The reason for doing so was to avoid a non-linear inequality coupling decision variables. Should I specify this justification?

(Integer Constraint Relaxed) Naive Brute Force Full Optimization Model - Full Horizon

C. ENApp based Distributed Multi-Period OPF with Batteries

III. Case Study Demonstration

A. Simulation Data: IEEE 123 Bus Test System

We're using a Balanced Three-Phase version of the IEEE 123 Bus Test System, which has 85 Load Nodes. Additionally, 20% (17) and 30% (26) of these load nodes also contain reactive power controllable Solar photovolatics (PVs) and Batteries respectively. Their ratings are as per Table II. To demonstrate the effectiveness of the proposed algorithm, the Test System has been divided into four areas on similar lines as [13]. The full test system along with the area-wise division is shown in Figure 1.

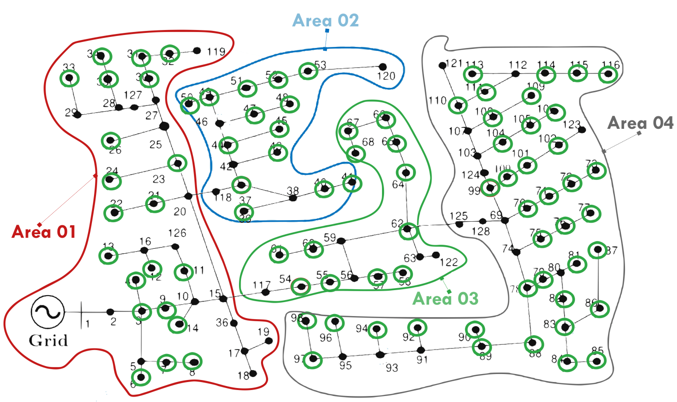

Fig. 1: IEEE 123 Node System Divided Into Four Areas

Change figure to display battery buses and PV buses

To showcase the workflow of the proposed algorithm, simulations were run for a 5 time-period horizon. Figure 2 shows the forecasted profiles for load, solar irradiance and cost of substation power over the horizon.

TABLE II: Parameter Values

Parameter	Value
V_{min}, V_{max}	0.95, 1.05
$p_{D_{R_j}}$	$0.33p_{L_{R_j}}$
$S_{D_{R_j}}$	$1.2p_{D_{R_j}}$
$P_{B_{R_j}}$	$0.33p_{L_{R_j}}$
B_{R_j}	$T_{fullCharge} \times P_{B_{R_j}}$
$T_{fullCharge}$	4 h
Δt	1 h
η_C, η_D	0.95, 0.95
soc_{min}, soc_{max}	0.30, 0.95
α	0.001

B. Simulation Workflow

We use MATLAB 2023a to set up our simulations. This includes both the high level algorithms as well as calling the optimization solver. We use MATLAB's `fmincon` function

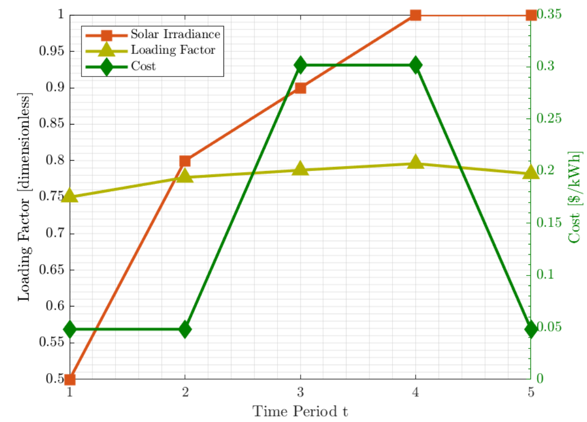

Fig. 2: Forecasts for Demand Power, Irradiance and Cost of Substation Power over a 5 Hour Horizon

to parse nonlinear nonconvex optimization problem described by (1) to (12) and the SQP optimization algorithm to solve it. Once the simulations are completed and resulting optimial control variables obtained, they are passed through an OpenDSS engine (which already has the known system data configured) in order to check for the feasiblity of the results.

C. Simulation Results

The Test System

1) Comparison between MPCOPF and MPDOPF: In this section, comparative analyses are carried out between MPCOPF and MPDOPF considering 5-hour time steps.

TABLE III: Comparative analyses between MPCOPF and MPDOPF - 5 time-period horizon

Metric	MPCOPF	MPDOPF
Biggest subproblem size		
Decision variables		
Linear constraints		
Nonlinear constraints		
Simulation results		
Substation power cost ($)	576.31	576.30
Substation real power (kW)	4308.28	4308.14
Line loss (kW)	75.99	76.12
Substation reactive power (kVAR)	574.18	656.24
PV reactive power (kVAR)	116.92	160.64
Battery reactive power (kVAR)	202.73	76.01
Computation		
Number of Iterations	-	5
Total Simulation Time (s)	521.25	49.87

Further, here the

Boundary Variable Plots are too tall, make them slightly shorter, like 25% of the page only.

D. Scalability Analysis

To demonstrate the effectiveness of the proposed algorithm over a bigger horizon to demonstrate scalability, simulations were run for a 10 time-period horizon. Figure 6 shows the forecasted profiles for load, solar irradiance and cost of substation power over the horizon.

TABLE IV: ACOPF feasibility analyses - 5 time-period horizon

Metric	MPDOPF	OpenDSS
Full horizon		
Substation real power (kW)	4308.14	4308.35
Line loss (kW)	76.12	76.09
Substation reactive power (kVAR)	656.24	652.49
Max. all-time discrepancy		
Voltage (pu)	0.0002	
Line loss (kW)	0.0139	
Substation power (kW)	0.3431	

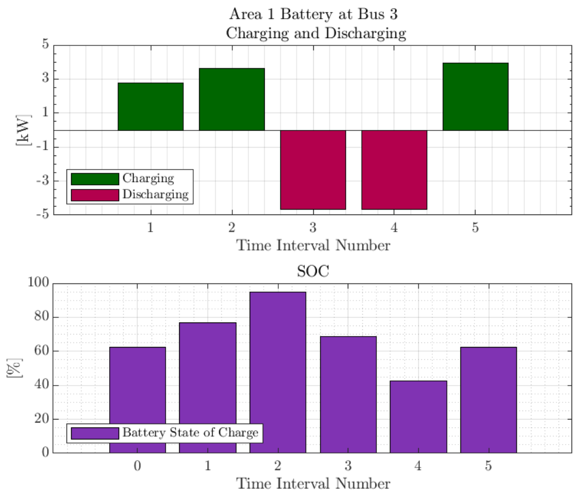

Fig. 3: Charging-Discharging and SOC graphs for Battery at Bus 3 located in Area 1 obtained by MPDOPF

1) Comparison between MPCOPF and MPDOPF: In this section, comparative analyses are carried out between MPCOPF and MPDOPF considering 10-hour time steps with 20% PV penetration and 30% battery penetration.

TABLE V: Comparative analyses between MPCOPF and MPDOPF - 10 time-period horizon

Metric	MPCOPF	MPDOPF
Biggest subproblem size		
Decision variables		
Linear constraints		
Nonlinear constraints		
Simulation results		
Substation power cost ($)	1197.87	1197.87
Substation real power (kW)	8544.28	8544.04
Line loss (kW)	148.67	148.94
Substation reactive power (kVAR)	1092.39	1252.03
PV reactive power (kVAR)	222.59	139.81
Battery reactive power (kVAR)	388.52	310.94
Computation		
Number of Iterations	-	5
Total Simulation Time (s)	4620.73	358.69

Further, here the

Lorem ipsum dolor sit amet, consectetuer adipiscing elit. Ut purus elit, vestibulum ut, placerat ac, adipiscing vitae, felis. Curabitur dictum gravida mauris. Nam arcu libero, nonummy eget, consectetuer id, vulputate a, magna. Donec vehicula

TABLE VI: ACOPF feasibility analyses - 10 time-period horizon

Metric	MPDOPF	OpenDSS
Full horizon		
Substation real power (kW)	8544.04	8544.40
Line loss (kW)	148.94	148.87
Substation reactive power (kVAR)	1252.03	1243.36
Max. all-time discrepancy		
Voltage (pu)	0.0002	
Line loss (kW)	0.0132	
Substation power (kW)	0.4002	

augue eu neque. Pellentesque habitant morbi tristique senectus et netus et malesuada fames ac turpis egestas. Mauris ut leo. Cras viverra metus rhoncus sem. Nulla et lectus vestibulum urna fringilla ultrices. Phasellus eu tellus sit amet tortor gravida placerat. Integer sapien est, iaculis in, pretium quis, viverra ac, nunc. Praesent eget sem vel leo ultrices bibendum. Aenean faucibus. Morbi dolor nulla, malesuada eu, pulvinar at, mollis ac, nulla. Curabitur auctor semper nulla. Donec varius orci eget risus. Duis nibh mi, congue eu, accumsan eleifend, sagittis quis, diam. Duis eget orci sit amet orci dignissim rutrum.

IV. Conclusions

[14], [15], [17]–[19]

References

[1] T. Gangwar, N. P. Padhy, and P. Jena, "Storage allocation in active distribution networks considering life cycle and uncertainty," IEEE Trans. Ind. Inform., vol. 19, no. 1, pp. 339–350, Jan. 2023.

[2] S. Paul and N. P. Padhy, "Real-time advanced energy-efficient management of an active radial distribution network," IEEE Syst. J., vol. 16, no. 3, pp. 3602–3612, Sept. 2022.

[3] W. Wei, J. Wang, and L. Wu, "Distribution optimal power flow with real-time price elasticity," IEEE Trans. Power Syst., vol. 33, no. 1, pp. 1097–1098, Jan. 2018.

[4] M. M.-U.-T. Chowdhury, B. D. Biswas, and S. Kamalasadan, "Second-order cone programming (socp) model for three phase optimal power flow (opf) in active distribution networks," IEEE Transactions on Smart Grid, vol. 14, no. 5, pp. 3732–3743, 2023.

[5] Z. Guo, W. Wei, L. Chen, Z. Dong, and S. Mei, "Parametric distribution optimal power flow with variable renewable generation," IEEE Trans. Power Syst., vol. 37, no. 3, pp. 1831–1841, May 2022.

[6] H. Yuan, F. Li, Y. Wei, and J. Zhu, "Novel linearized power flow and linearized opf models for active distribution networks with application in distribution lmp," IEEE Trans. Smart Grid, vol. 9, no. 1, pp. 438–448, Jan. 2018.

[7] A. R. Di Fazio, C. Risi, M. Russo, and M. De Santis, "Decentralized voltage optimization based on the auxiliary problem principle in distribution networks with ders," Appl. Sci., vol. 11, no. 4509, pp. 1–24, 2021.

[8] W. Zheng, W. Wu, B. Zhang, H. Sun, and Y. Liu, "A fully distributed reactive power optimization and control method for active distribution networks," IEEE Trans. Smart Grid, vol. 7, no. 2, pp. 1021–1033, Mar. 2016.

[9] P. Wang, Q. Wu, S. Huang, C. Li, and B. Zhou, "Admm-based distributed active and reactive power control for regional ac power grid with wind farms," J. Modern Power Syst. Clean Energy, vol. 10, no. 3, pp. 588–596, May 2022.

[10] B. D. Biswas, M. S. Hasan, and S. Kamalasadan, "Decentralized distributed convex optimal power flow model for power distribution system based on alternating direction method of multipliers," IEEE Trans. Ind. Appl., vol. 59, no. 1, pp. 627–640, Jan.-Feb. 2023.

[11] A. Gabash and P. Li, "Active-reactive optimal power flow in distribution networks with embedded generation and battery storage," IEEE Trans. Power Syst., vol. 27, no. 4, pp. 2026–2035, Nov. 2012.

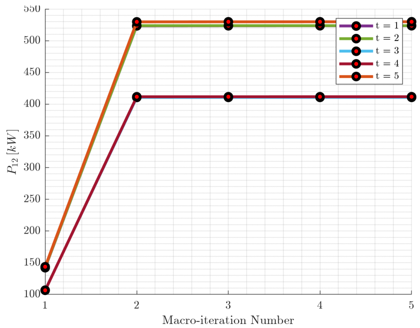

(a) Real Power flowing from Area 1 into Area 2

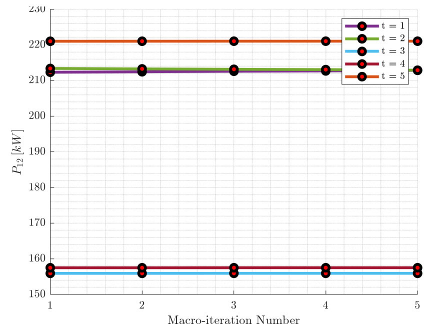

(b) Real Power flowing from Area 1 into Area 3

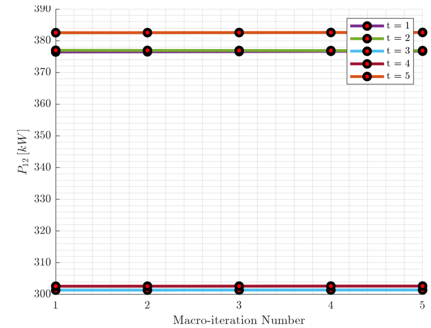

(c) Real Power flowing from Area 2 into Area 4

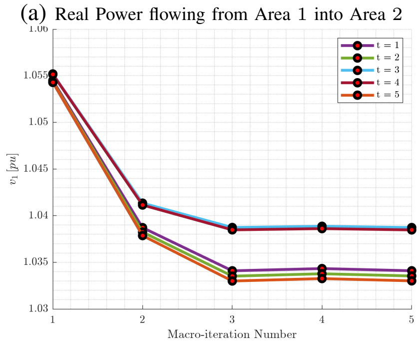

(d) Voltage at the PoI of Area 1 and Area 2

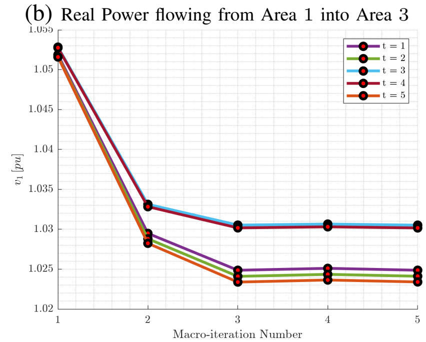

(e) Voltage at the PoI of Area 1 and Area 3

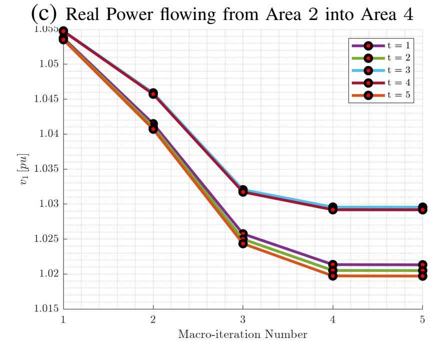

(f) Voltage at the PoI of Area 2 and Area 4

Fig. 4: Convergence of Boundary variables with every iteration. Each plot represents a particular variable exchanged between a pair of connected areas. Each line graph within a plot represents a particular time period.

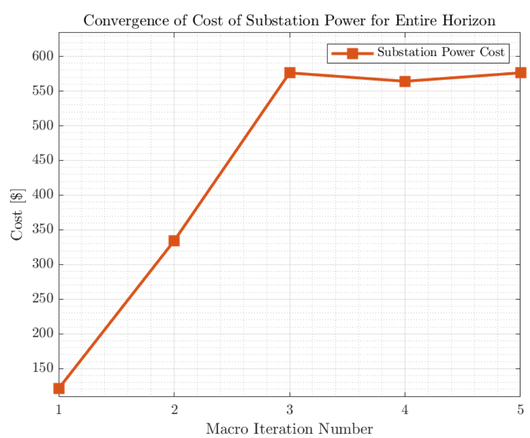

Fig. 5: Convergence of Objective Function Value with each MPDOPF iteration

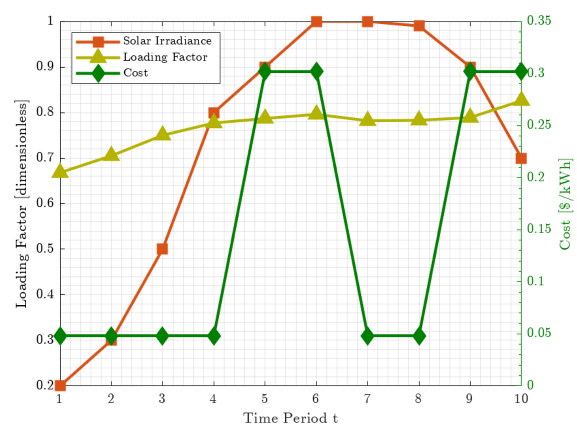

Fig. 6: Forecasts for Demand Power, Irradiance and Cost of Substation Power over a 10 Hour Horizon

[12] C. Wu, W. Gu, S. Zhou, and X. Chen, "Coordinated optimal power flow for integrated active distribution network and virtual power plants using decentralized algorithm," IEEE Trans. Power Syst., vol. 36, no. 4, pp. 3541–3551, Jul. 2021.

[13] R. Sadnan and A. Dubey, "Distributed optimization using reduced network equivalents for radial power distribution systems," IEEE Trans. Power Syst., vol. 36, no. 4, pp. 3645–3656, Jul. 2021.

[14] N. Nazir and M. Almassalkhi, "Receding-Horizon Optimization of Unbalanced Distribution Systems with Time-Scale Separation for Discrete and Continuous Control Devices," pp. 1–7, Jun. 2018.

[15] N. Nazir, P. Racherla, and M. Almassalkhi, "Optimal multi-period dispatch of distributed energy resources in unbalanced distribution feeders," Jun. 2019.

[16] N. Nazir and M. Almassalkhi, "Guaranteeing a Physically Realizable Battery Dispatch Without Charge-Discharge Complementarity Constraints," IEEE Trans. Smart Grid, vol. 14, no. 3, pp. 2473–2476, Sep. 2021.

[17] M. Farivar and S. H. Low, "Branch flow model: Relaxations and convexification," 2012 IEEE 51st IEEE Conference on Decision and Control (CDC), pp. 3672–3679, Dec. 2012.

[18] A. Agarwal and L. Pileggi, "Large Scale Multi-Period Optimal Power Flow With Energy Storage Systems Using Differential Dynamic Programming," pp. 1750–1759, Sep. 2021.

[19] X. Qian and Y. Zhu, "Differential Dynamic Programming for Multistage Uncertain Optimal Control," pp. 88–92, Jul. 2014.

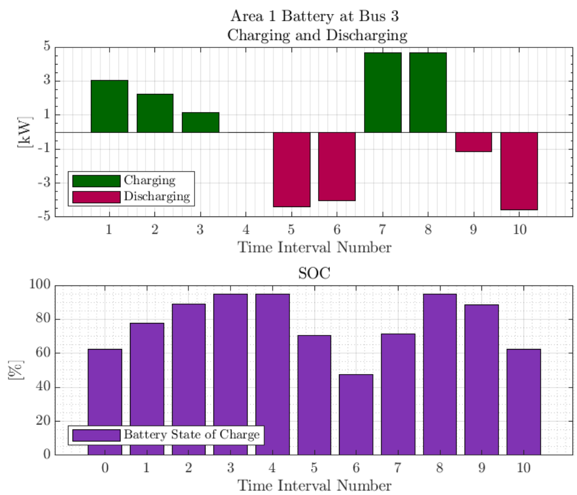

Fig. 7: Charging-Discharging and SOC graphs for Battery at Bus 3 located in Area 1 obtained via MPDOPF